Inorganic Chemistry

pubs.acs.org/IC Article

Bis-tridentate N-Heterocyclic Carbene Ru(II) Complexes are Promising New Agents for Photodynamic Therapy

Raphael T. Ryan, Kimberly C. Stevens, Rosemary Calabro, Sean Parkin, Jumanah Mahmoud, Doo Young Kim, David K. Heidary, Edith C. Glazer,* and John P. Selegue*

Cite This: *Inorg. Chem.* 2020, 59, 8882–8892 Read Online

ACCESS | Metrics & More | Article Recommendations | Supporting Information

ABSTRACT: Ruthenium(II) complexes developed for photodynamic therapy (PDT) are almost exclusively tris-bidentate systems with C_2 or D_3 symmetry. This is due to the fact that this structural framework commonly produces long-lived excited states, which, in turn, allow for the generation of large amounts of singlet oxygen ($^1O_2$) and other reactive oxygen species. Complexes containing tridentate ligands would be advantageous for biological applications as they are generally achiral (D_{2d} or C_{2v} symmetry), which eliminates the possibility of multiple isomers which could exhibit potentially different interactions with chiral biological entities. However, Ru(II) complexes containing tridentate ligands are rarely studied as candidates for photobiological applications, such as PDT, since they almost exclusively exhibit low quantum yields and very short excited-state lifetimes and, thus, are not capable of generating sufficient $^1O_2$ or engaging in electron transfer reactions. Here, we report a proof-of-concept approach to make bis-tridentate Ru(II) complexes useful for PDT applications by altering their photophysical properties through the inclusion of N-heterocyclic carbene (NHC) ligands. Three NHC and two terpyridine ligands were studied to evaluate the effects of structural and photophysical modulations of bis-substituted Ru(II) complexes. The NHC complexes were found to have superior excited-state lifetimes, $^1O_2$ production, and photocytotoxicity. To the best of our knowledge, these complexes are the most potent light-activated bis-tridentate complexes reported.

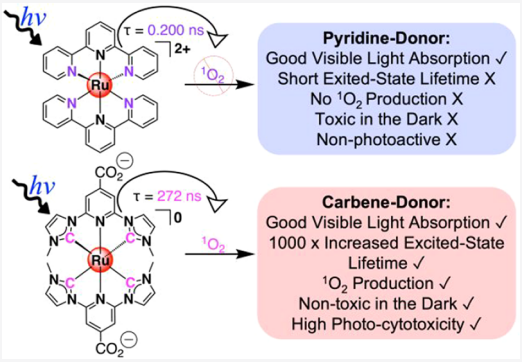

INTRODUCTION

Photodynamic therapy (PDT) is an FDA-approved cancer treatment where a nontoxic photoactivatable drug, a light source, and cellular oxygen combine to induce cell death via production of singlet oxygen ($^1O_2$) and other cytotoxic reactive oxygen species (ROS).[1] Despite notable clinical successes of PDT, the tetrapyrrole macrocycle agents currently used for PDT suffer limitations, including low solubility[2] and slow clearance from the body, causing patients to become light sensitive for extended periods.[1] As alternative PDT agents have been explored,[3] ruthenium(II) polypyridyl complexes have come to prominence as photosensitizers[3c,4] as they have many desired properties for PDT. These include tunable hydrophilicity,[5] favorable photophysics, and visible-light absorbance.[6] The advantages of this class of Ru(II) complexes have been recently demonstrated by the successes of TLD-1433, a Ru(II) complex which has entered international, multicenter phase II trials for treatment of nonmuscle invasive bladder cancer.[7]

Investigations of Ru(II) complexes for PDT have primarily focused on tris-bidentate analogs of $[Ru(bpy)_3]^{2+}$ (bpy = 2,2′-bipyridine)[3c,4a,c] of D_3 or C_2 symmetry, for homo- or heteroleptic complexes, respectively. The archetypical tris-bidentate ligand framework is used almost exclusively since it allows for easy structural modification and results in triplet metal-to-ligand charge transfer (^{3}MLCT) excited states with lifetimes (τ) approaching or exceeding the microsecond time scale.[4c,6b] The long-lived ^{3}MLCT state is vital to allow ample time for energy or electron transfer to take place between the metal complex and cellular species.[8] Notably, some of the most effective light-activated agents contain organic moieties that allow for equilibration of the ^{3}MLCT state with an interligand excited state (^{3}IL), producing lifetime in the hundreds of microseconds.[9]

In contrast, there are only a limited number of examples of Ru(II) complexes with tridentate ligands that have been studied as potential PDT agents.[10] The disproportionate use of bidentate ligands is due to the fact that the majority of complexes with tridentate ligands possess inherently poor photophysics, including short-lived ^{3}MLCT states. The prototypical bis-tridentate Ru(II) complex, $[Ru(tpy)_2]^{2+}$ (tpy

Received: March 6, 2020
Published: June 12, 2020

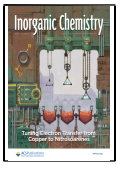

© 2020 American Chemical Society

https://dx.doi.org/10.1021/acs.inorgchem.0c00686
Inorg. Chem. 2020, 59, 8882–8892

Chart 1. Compounds Studied in this Report

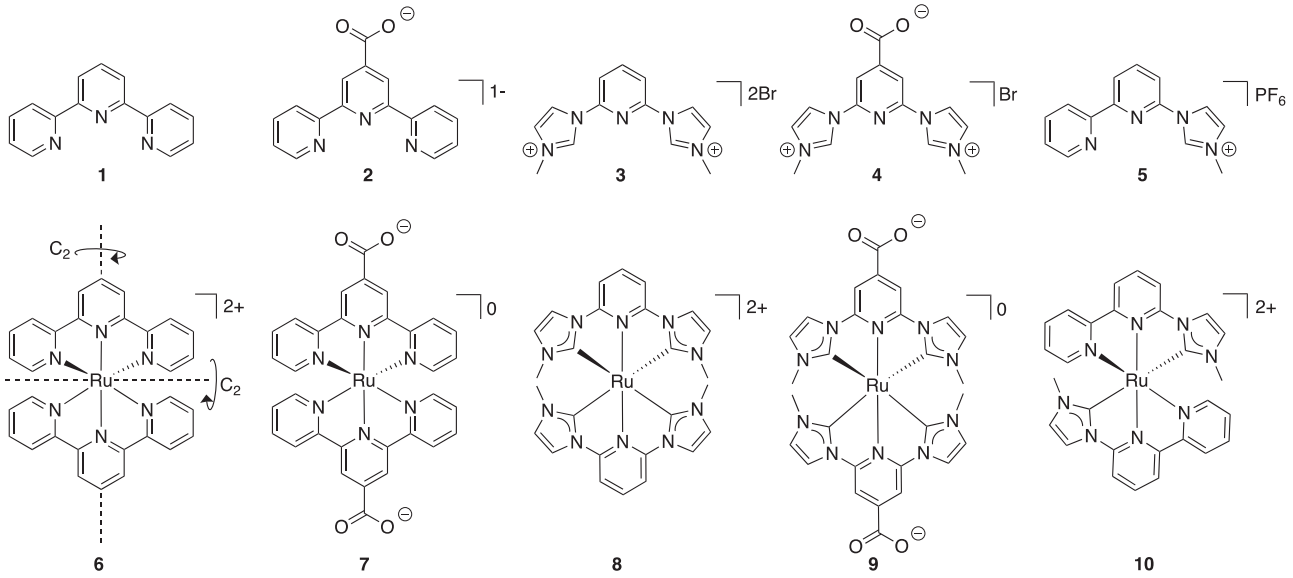

= 2,2′:6′,2″-terpyridine) highlights the difficulty of using tridentate complexes because its short-lived excited state (τ = 0.250 or 0.200 ns in water under argon[11] or air, respectively) makes it practically unusable for PDT. A significant number of $[Ru(tpy)_2]^{2+}$ analogs have been synthesized with the goal of improving photophysical properties, but many of these still do not possess excited states exceeding 60 ns even when measured under favorable conditions, such as in degassed acetonitrile[12] or in the solid state.[13]

The short-lived excited state of $[Ru(tpy)_2]^{2+}$ and related complexes arises from the weak ligand field induced by deviation from an ideal octahedral geometry imposed by the tridentate ligands. Upon photoexcitation, these complexes populate the ^{3}MLCT state, but this is rapidly followed by thermal population of the nonemissive, antibonding triplet metal-centered (^{3}MC) state. The ^{3}MC state quickly relaxes to the ground state, preventing the energy and/or electron transfer reactions that normally occur from the ^{3}MLCT state to form ROS.[6b,12] Unlike the distorted Ru(II) bidentate complexes that we previously developed, which release a ligand when the ^{3}MC state is populated,[6b,14] the tridentate chelate ligand is not ejected upon ^{3}MC population. Thus, these systems are not useful for either photocatalytic processes or photoreactions following ligand release.

Compounds with structures similar to $[Ru(tpy)_2]^{2+}$ with long-lived ^{3}MLCT states would be advantageous for many applications because they are usually achiral (often D_{2d} or C_{2v} symmetry), which is ideal for purposes where chirality should be limited or eliminated altogether. For example, there is great interest in such systems as light harvesting supramolecular arrays.[12,15] The achiral nature of these kinds of complexes is also desirable for metal-based drugs because significant differences in biological activity have been reported for enantiomers and diastereomers of metal complexes.[16] While enantiomerically pure complexes can increase specificity and selectivity compared to a racemic mixture,[16b] their chiral resolution can be tedious to pursue[17] or require specialized instrumentation,[18] which complicate their use. Ru(II) tris-bidentate complexes generally exist as a mixture of Δ and Λ enantiomers, and *cis* and *trans* isomers are possible if one of the bidentate ligands is lost, resulting in unwanted chiral complexity.

Several methods have been explored to modulate the tpy ligand framework to prepare tridentate complexes with long-lived ^{3}MLCT states.[12,15a,19] However, to the best of our knowledge, only three strategies have been evaluated to make photoactive bis-tridentate complexes useful for biological applications. The first approach took advantage of tridentate ligands with extended π-conjugated frameworks, which produced a long-lived ligand-centered excited state. This resulted in complexes with $^1O_2$ quantum yields (Φ_Δ) of approximately 1[20] for heteroleptic and homoleptic metal complexes.[10b] The complexes induced very efficient photocleavage of plasmid DNA[10b] and photo-cross-linked the protein p53 to give dimers, trimers, and tetramers.[10a] However, no values for dark cytotoxicity were reported.[10a,b] The second method utilized a ligand with an expanded chelate bite angle that approached the ideal octahedral angles of 90° and 180° for *cis* and *trans* coordination sites. The complex possessed a longer excited state lifetime (τ = 12 ns in aerated toluene) and a light-activated inhibitory concentration for 50% loss in viability (IC_{50}) value of 25.3 μM in HeLa cells.[10c] However, the phototoxicity index (PI; the ratio of cytotoxicity IC_{50} values with and without photoactivation) was only 4. The last method modified electronic properties by appending different electron withdrawing or donating groups to the 4′ position of one tpy ligand in bis-heteroleptic tpy complexes.[10d] These complexes had short excited-state lifetimes that were outside the authors' capability to measure but were estimated to be <29 ns in degassed acetonitrile. One complex exhibited an IC_{50} of 24.5 μM with exposure to light; however, with PI = 1.4, this complex was not promising for PDT. This study suggested that the addition of electron withdrawing or donating groups to one tpy ligand is not a viable methodology for PDT agents due to their short lifetimes and poor phototoxicity.

Here, we report an alternative design strategy for the creation of phototoxic tridentate ruthenium complexes. We chose to replace the tpy ligands with ligands that would be structurally analogous but would also be intrinsically electronically distinct in order to give longer lived ^{3}MLCT states without the need for many structural modifications. N-

https://dx.doi.org/10.1021/acs.inorgchem.0c00686
Inorg. Chem. 2020, 59, 8882−8892

Table 1. Photophysical Data for Complexes 6−10[a]

complex	λ_{max}^{abs} (nm) (ε, 10^3 M^{-1} cm^{-1})	λ_{max}^{em} (nm)[c]	$\varepsilon_{405\ nm}$ (10^3 M^{-1} cm^{-1})[c]	$\varepsilon_{450\ nm}$ (10^3 M^{-1} cm^{-1})[c]	τ (ns)[l]	$E_{1/2}^{2+/3+}$ (V, vs NHE)
6	475 (17.2),[b] 475 (15)[c]	617	3.6	10	0.200 ± 0.001,[c]0.250[e]	1.55[h]
7	495 (21),[b] 485 (27)[d]	653	4.5	13	4.5 ± 0.02[c]	1.65[j]
8	382 (16),[b] 380 (19)[c]	532	5.1	1.2	529 ± 0.6[c]	1.38[h]
9	430 (26),[b] 415 (20)[c]	610	17.3	3.8	272 ± 0.3[c]	1.78[I]
10	465 (9.8),[b] 460 (7.5)[c]	622	3.8	6.0	107 ± 0.01[c]	1.43[h]
$[Ru(bpy)_3]^{2+}$	450 (14.3),[b,f] 452 (14.0)[c,g]	627	7.1	14	376 ± 0.4[c]	1.26[k]

[a]All photophysical measurements were obtained under air at room temperature. [b]Measured in MeCN. [c]Measured in water (pH ∼ 9).[21] [d]Measured in water with ∼0.2% methanol. [e]From ref 11, measured in degassed water. [f]From ref 19d. [g]From ref 6a. [h]From ref 22. [I]From ref 23. [j]From ref 24. [k]From ref 6b. [l]Luminescence excited-state lifetimes are referred to as excited-state lifetimes.

Heterocyclic carbenes (NHCs) were chosen as the ideal ligands to evaluate as tpy replacements because they are strong σ-donors with a demonstrated capacity to dramatically increase excited state lifetimes of tridentate Ru(II) complexes[19a,d,25] by destabilizing the ^{3}MC state, reducing its population from the ^{3}MLCT state.[12,15a] Additionally, the neutral character of NHC ligands in metal complexes[26] is also beneficial to this study as they maintain an overall 2+ charge, making them more similar to $[Ru(tpy)_2]^{2+}$ than other strong σ-donors, such as cyclometalated ligands, which are anionic and reduce the overall charge on the complex. Cyclometalated Ru(II) complexes are often toxic in the absence of light, reducing their suitability for PDT.[27] While NHC complexes have been studied as potential chemotherapeutics,[28] photobiological investigations have been limited to a few examples of Ir(III) and Pt(II) complexes,[29] with no examples of Ru(II) complexes until now.

We utilized the electron donating ability of the NHC ligands to produce homoleptic Ru(II) complexes for evaluation as potential PDT agents. The replacement of tpy ligands with structurally analogous NHCs provides complexes with exceptional excited state lifetimes (up to ∼ 2600-fold higher than $[Ru(tpy)_2]^{2+}$). The complexes successfully generated $^1O_2$, while $[Ru(tpy)_2]^{2+}$ does not. Moreover, the NHC complexes were completely nontoxic in the dark and exhibited low micromolar cytotoxicity upon irradiation, in marked contrast to $[Ru(tpy)_2]^{2+}$, making them useful scaffolds for PDT.

RESULTS AND DISCUSSION

Synthesis and Characterization. To evaluate the hypothesis that strong σ-donor NHC ligands could improve photophysical and photobiological properties, five bis-homoleptic tridentate Ru(II) complexes (compounds **6−10**) were synthesized and studied, i.e., two containing terpyridine (**1** and **2**) and three containing NHC ligands (**3−5**; Chart 1). All complexes were isolated at ≥95.7% purity as determined by HPLC and were characterized by ^{1}H and ^{13}C NMR, ESI mass spectrometry, and UV−vis spectroscopy. Structural analysis was performed by X-ray crystallography (for complexes **8−10**) and compared to reported structures of **6**,[30] **8**[19d,31] (as its BPh_4^- and BF_4^- salts),[32] and other tridentate Ru(II) NHC complexes.[33] Complexes **6** and **7** were synthesized as control compound analogues to complexes **8** and **9**.

Both compounds **7** and **9** contain carboxylic acids, which added complications. The protonated form of **7** is known to be difficult to handle due to its low solubility and the tendency to lose HPF_6 in solution and upon drying in vacuo[24] to give a mixture of a poorly soluble dark brown solid intertwined with a more soluble red solid. Other Ru(II) complexes containing carboxylic acids with PF_6^- counterions have also shown this instability.[34] All efforts were made to prevent this loss of HPF_6 so the complex could be converted to the Cl^- salt, but it is possible that trace amounts remained. Additionally, a dark brown solid slowly precipitated from water and acetonitrile solutions of **7** over time. Notably, no similar effects were observed for complex **9**. However, spectroscopic characterization was performed at pH ∼9 to prevent solution heterogeneity and altered emission properties, such as proton-induced excited state quenching.[35]

Complexes **8−10** provide structures with differences in the number of NHC groups, chirality, and overall charge on the complex. The high-energy, ligand-based lowest unoccupied molecular orbitals (LUMO) of NHC complexes are known to shift the absorption of Ru(II) complexes into the ultraviolet region.[19d,22,23,36] As anticipated, complex **8** barely absorbs visible light (λ_{max} = 380 nm) compared to **6** (λ_{max} = 475 nm, Table 1, Figure 1). This hypsochromic shift makes **8** ill-suited for biological applications because the high-energy light required for activation can directly damage tissue.[4a] Both complexes **9** and **10** were chosen[22,23] with strategic structural variations to alter the visible-light absorbance of each complex relative to **8** by lowering the energy of the molecular orbitals

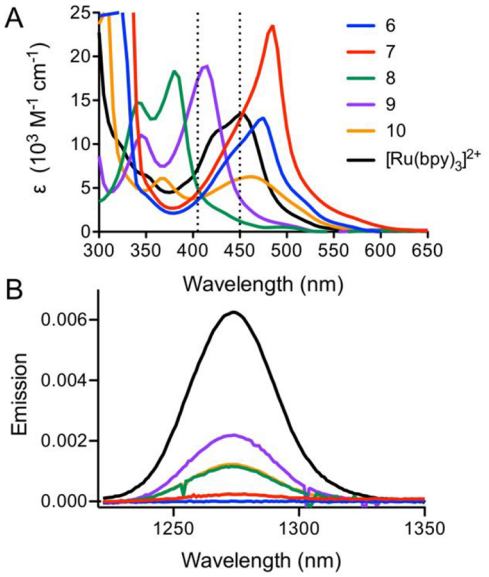

Figure 1. (A) Absorbance spectra for **6−10** and $[Ru(bpy)_3]^{2+}$ in water. Vertical lines mark 405 nm and 450 nm. (B) Measurement of $^1O_2$ phosphorescence generated by **6−10** and $[Ru(bpy)_3]^{2+}$ in CD_3OD (λ_{ex} = 450 nm). All samples were isoabsorptive (A ∼ 0.2) at 450 nm, except for **8** (green), which was measured at a concentration of 100 μM.

https://dx.doi.org/10.1021/acs.inorgchem.0c00686
Inorg. Chem. 2020, 59, 8882−8892

on the ligands. This was accomplished by expanding the electronic delocalization over each ligand by either the attachment of a carboxylic acid to the pyridyl ring[23] (**9**) or the replacement of a carbene ring with a second pyridyl ring (**10**).[22] These modifications resulted in visible light absorption (λ_{max} = 415 and 460 nm for **9** and **10** in water), along with notable 4−5-fold increases in ε_{450} compared to that of **8** (Table 1, Figure 1A). Complexes **6**−**9** are achiral (D_{2d} symmetry) while complex **10** is chiral (C_2 symmetry). Despite complex **10** being chiral, it was included in this study to probe the photophysical and biological effect of including two NHC groups versus the four contained in **8**−**9**.

X-ray Crystallography. The structures of **8**−**10** were determined by X-ray crystallography (Figure 2, Table 2, Tables S1−S5). Complex **9** crystallized as the monocation with one acid group deprotonated. The deprotonation results in molecules of **9** being ordered into an hydrogen bonded array along the [−1 0 1] direction between H4A and O1 on separate molecules via "short−strong" hydrogen bonds (SSHBs, hydrogen bonds which are unusually short, with distances between the donor and acceptor oxygen atoms less than 2.55 Å).[37] The short distance (2.482 Å) indicates strong hydrogen bonding between complexes, which could potentially also occur between the complex and molecules (such as proteins) within cells.

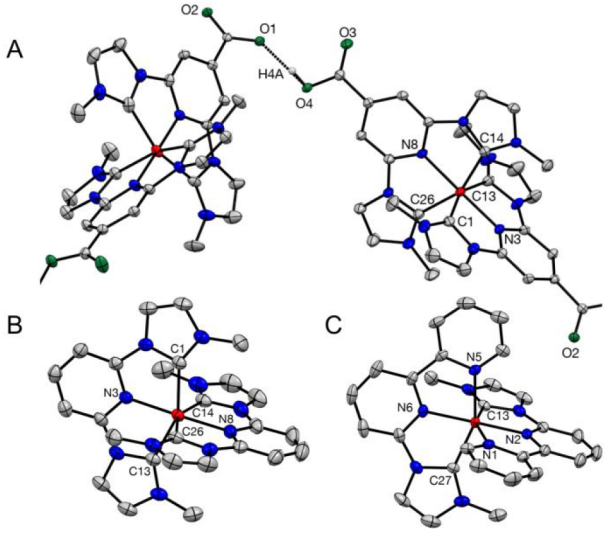

Figure 2. Ellipsoid plots of (A) compound **9** showing hydrogen bonding between adjacent molecules, (B) **8**, and (C) **10** at 50% probability. Non-hydrogen bonding H atoms and counterions are omitted for clarity.

Table 2. Selected Bond Lengths (Å) and Bond Angles (deg) for 8 and 9

bond length (Å)	complex **8**[a]	complex **9**
Ru1−C1	2.0531(19)	2.047(3)
Ru1−C13	2.0524(19)	2.056(2)
Ru1−C14	2.0475(19)	2.046(2)
Ru1−C26	2.0489(19)	2.054(3)
Ru1−N3	2.0156(16)	2.0106(19)
Ru1−N8	2.0149(17)	2.0076(19)
O4−H4A	n/a	0.8400
O1−H4A	n/a	1.657
O1−O4	n/a	2.482
bond angle (deg)	complex **8**	complex **9**
C13−Ru1−C	153.92(8)	153.86(10)
C14−Ru1−C26	154.05(9)	153.99(13)

[a]n/a = not applicable.

The structures of **8**−**10** all resembled **6**[30] as they formed the expected distorted octahedral tridentate *mer*-isomers. The *trans*-NHC−NHC or NHC−pyridine angles of **8**−**10** are in the range of 153.86−156.00° (Table 2 and Table S5), deviating significantly from the ideal 180° *trans* angle. Notably, this is a larger distortion than the average *trans* pyridine−pyridine angle of 158.4° in **6**.[30b] The central Ru−$N_{pyridyl}$ bond lengths of **8**−**10** ranged from 2.002 to 2.016 Å, which is slightly longer than the 1.976 Å average bond of the central Ru−$N_{pyridyl}$ bond for **6**.[30a] In contrast, the Ru−$N_{pyridyl}$ bond *trans* to the strongly electron-donating Ru−$C_{carbene}$ in **10** reflects a *trans* influence, which increases the length to an average 2.130 Å. The Ru−$C_{carbene}$ bond lengths of **8** and **9** are 2.050 Å (average), which are slightly shorter than the 2.067 Å *trans* N-bonds of **6**.[30b] The Ru−$C_{carbene}$ bonds of **10** are 1.999 Å (average), shorter than those in **8** or **9** due to the weaker *trans* influence of the pyridyl donor. The structures are very similar to other Ru(II) NHC complexes[19d,31,33] and show that the presence of the NHC ligands does not result in better-optimized bond lengths or angles compared to tpy Ru(II) complexes.

Excited-State Lifetime Measurements. Excited-state lifetimes for complexes **6**−**10** were measured by time-correlated single photon counting (TCSPC; Table 1, Figure S2). The compounds were studied in air-equilibrated water to model their behavior under biological conditions.[38] Gratifyingly, complexes **8**−**10** all exhibited lifetimes that were 535−2645-fold greater than the lifetime measured for **6** (τ = 0.200 ns). Moreover, these excited-state lifetime values are ∼3.7−44-fold greater than those of previously reported tpy-based complexes evaluated for PDT applications,[10c,d] demonstrating the importance of NHC-based ligands compared to weakly donating tpy ligands.

Despite the similar structures of **8**, **9**, and **10**, their excited-state lifetimes exhibited a large range. Complex **8** had the longest excited-state lifetime (τ = 529 ns),[39] which is over 2000-fold greater than that of **6**. In comparison, the lifetime of **9** (τ = 272 ns) was about half that of **8**. This is surprising for two reasons. (1) Compounds **8** and **9** have statistically equivalent bond distances and angles between the ligands and the metal center and only differ due to the carboxylate groups of **9**. (2) The addition of electron-withdrawing or -donating groups to tpy complexes generally *increases* excited-state lifetimes by stabilizing the LUMO or destabilizing the HOMO, respectively.[10d,12] Indeed, the introduction of carboxylates to the analogous terpyridine complex, **7**, resulted in an *increased* lifetime (τ = 4.5 ns) relative to **6** (τ = 0.2 ns). However, the opposite effect was found with the NHC ligand. This difference may be due to the electronic effects caused by the carboxylate being different for each complex. The longer lifetime for **7** is likely due to a relatively larger ^{3}MLCT−^{3}MC gap due to the donor ability of the carboxylate destabilizing the HOMO. Since the energy of the ^{3}MC is likely higher for **9** than for **7**, the shorter lifetime of **9** may be related to the energy-gap law.[12] The energy-gap law predicts, correctly, in this case, that decreasing the emission energy from 532 nm for **8** to 610 nm for **9** will be accompanied by an increased rate of nonradiative

https://dx.doi.org/10.1021/acs.inorgchem.0c00686
Inorg. Chem. 2020, 59, 8882−8892

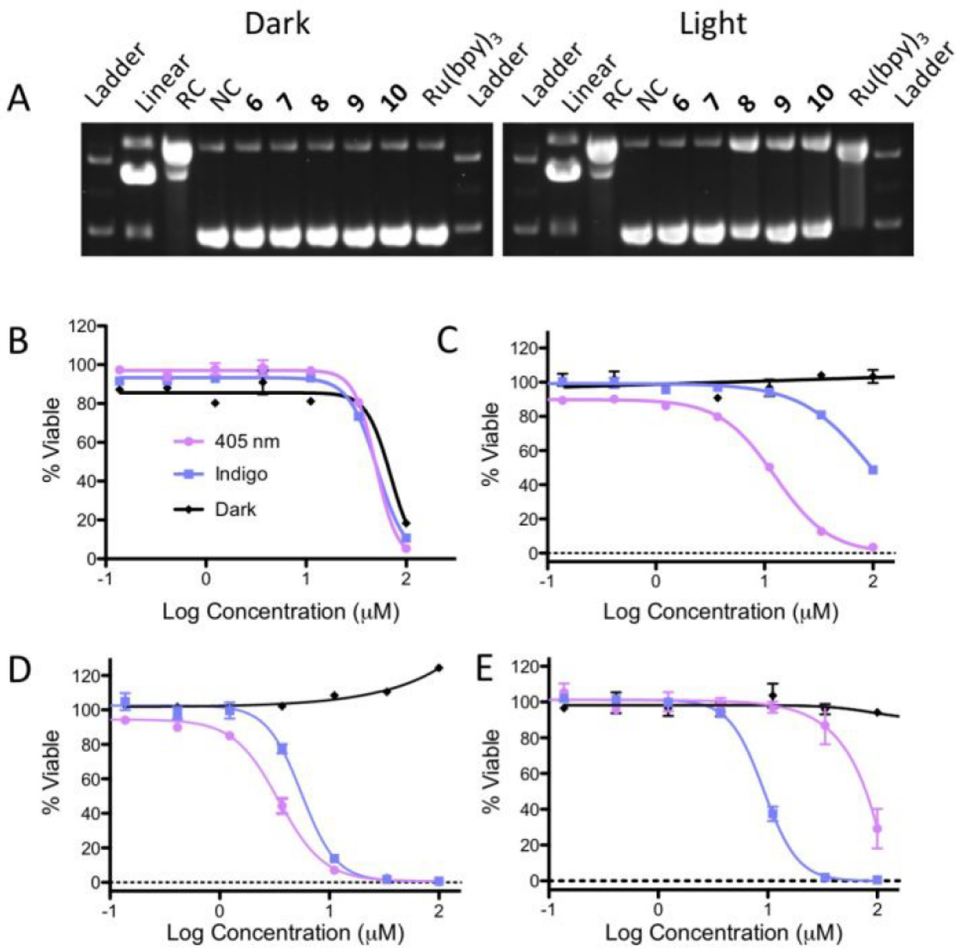

Figure 3. (A) Agarose gel electrophoresis of pUC19 plasmid (40 μg mL^{-1}, 10 mM phosphate buffer, pH 7.4) under dark conditions (left) and after irradiation (right; 470 nm light, 37 J cm^{-2}). All compounds were tested at 500 μM; RC = relaxed circle, NC = no compound. Cytotoxicity dose responses in HL 60 cells: (B) **6**, (C) **8**, (D) **9**, and (E) **10**. Dark conditions (black diamonds), following irradiation with 405 nm (lavender squares) and 450 nm light (orchid circles) (n = 3).

decay and decreased ^{3}MLCT lifetime due to increased vibronic coupling between the ^{3}MLCT and ground states.[40]

The excited-state lifetime of **10** (τ = 107 ns) was the shortest of the Ru-NHC complexes and was associated with a decrease in the number of NHC−metal bonds, from four to two, for **10** relative to **8** and **9**. This structural change in **10** also results in a lower energy emission (622 nm) which, relative to **8** and **9**, also follows the energy-gap law.[12] Overall, compounds **8**−**10** exhibited vastly improved lifetimes compared to **6** and **7**, with complex **8** having a longer lifetime than the benchmark D_3 complex, $[Ru(bpy)_3]^{2+}$, under the experimental conditions used (τ = 376 ns, Table 1). The enhanced lifetimes for **8**−**10** were very promising for their application as PDT agents and gives these complexes a distinct advantage compared to **6**[11] and other terpyridine Ru(II) complexes[12] and PDT agents.[10c,d]

Electrochemical Analysis. As the crystal structures did not fully explain the donor capability of these complexes, insights were sought from their electrochemical behavior. The extent of the ^{3}MC state destabilization due to ligand field effects is important to these systems, so the ligand donor strength was considered in the context of the first oxidation potentials of **6**−**10**.[41] The oxidation potential of **7** (1.65 V vs NHE) reflects that 2,2′:6′,2″-terpyridine-4′-carboxylic acid in **7** is a weaker donating ligand than the 2,2′:6′,2″-terpyridine ligand in **6** (1.55 V vs NHE), as indicated by the more positive potentials. The carboxylic acid NHC ligand in **9** appears to be an even weaker donor ligand. Interestingly, there is a 0.40 V difference between the first oxidation potential of **8** (1.38 V) and the protonated form of **9** (1.78 V), indicating a substantial modulation of the metal center HOMO of **9** as a result of the electron-withdrawing carboxylic acid groups. This difference in the first oxidation potential is 4-fold larger than that of **6** and **7** and demonstrates a greater effect of functional group additions on the NHC ligand.[23] The first oxidation potentials of the protonated forms of **7** (1.65)[42] and **9** (1.78 V)[23] are similar, suggesting that **2** and **4** (when protonated) are both weaker electron-donating ligands than **1**.

While the ligand donor strength is likely an important component that impacts the long-lived excited-states seen for **8**−**10**, the excited-state lifetimes do not scale with the metal center redox potentials for these compounds. This is very clear when comparing **8**, which has the least positive oxidation potential (reflecting strongly electron-donating ligands) and the longest excited-state lifetime, and **9**, which has the most positive potential but still has the second longest lifetime. However, compound **9** is an outlier, as a low oxidation potential has been associated with long excited-state lifetimes for other tridentate NHC complexes.[19a,25] This relationship, and its pH dependence, merits further study to understand how it relates to other properties, such as MLCT energy.

https://dx.doi.org/10.1021/acs.inorgchem.0c00686
Inorg. Chem. 2020, 59, 8882−8892

Table 3. Cytotoxicity Data for 6−10 in HL60 Cells with 405 nm and Indigo (~450 nm) Light Sources

	IC_{50} ± standard deviation (μM)			phototoxicity index (PI)	
compound	dark	405 nm	indigo	405 nm	indigo
6	~65	~50	~50	~1.3	~1.3
7	>100	>100	>100	N/A	N/A
8	>300	12.5 ± 0.5	~100	>24	>3
9	>300	3.5 ± 0.5	5.6 ± 0.2	>86	>54
10	>300	~70	9.1 ± 1	>4.3	>37
$[Ru(bpy)_3]^{2+}$	>100	5.2 ± 1	0.3 ± 0.03	>19	>333
ALA[a]	>300	n.d.[b]	16.2 ± 3.2[b]	n.d.[b]	>18
cisplatin[a]	3.1 ± 0.2	n.d.[b]	3.4 ± 0.6[b]	n.d.[b]	1

[a]From ref 14a. [b]Blue light source; n.d. = not determined.

However, caution should be taken when attempting to apply electrochemical data to help rationalize the properties of complexes that are measured in aqueous environment. Redox potentials can vary between aqueous media and organic solvents, which makes comparison between different solvents challenging.[43] The redox potentials were not measured under biologically relevant aqueous conditions due to the narrow (−0.41−0.82 V vs NHE)[44] electrochemical window of water (pH = 7), which sets the upper limit below the range of our complexes. In addition, common biological buffers have also been demonstrated to have narrow windows that exclude them from use with these compounds.[45]

Complex Stability. The stability of PDT agents is an important characteristic due to the potential for decomposition to form cytotoxic byproducts. To evaluate the thermal stability of **8**−**10** under aqueous conditions, the complexes were incubated at 37 °C for 72 h and monitored by UV/vis spectroscopy. Solutions of varying complexity (Milli-Q-water, sodium chloride/HEPES buffer, and Opti-MEM with 2% fetal bovine serum) were investigated to assess the probability of the complexes interacting or reacting with the components found in tissue culture experiments, compared to water and buffer. The absorbance profiles (Figure S1) for all complexes in each solution remained essentially unchanged over the course of 72 h, indicating stable complexes suitable for biological applications.

The photostability was studied by monitoring the decrease of the MLCT absorbance peak by UV/vis during irradiation (470 nm, 37 J cm^{-2}; Figures S19 and S20, Table S7). The complexes were studied in water, TRIS HCl buffer (pH = 7.4), and Opti-MEM with 2% fetal bovine serum. All complexes showed good photostability, as demonstrated by MLCT absorbance decreases of <7% for each complex. The behavior of polypyridyl complexes **6**, **7**, and $[Ru(bpy)_3]^{2+}$ was similar, with all complexes remaining essentially unchanged (3% decrease) in each medium tested. Surprisingly, **8**−**10** showed the most degradation in pure water, with absorbance decreases of 4.4−6.3%. When studied in TRIS buffer and Opti-MEM, **8**−**10** showed better stability, with decreases of 0.29−3.6%. Overall, these data are promising as **8**−**10** are ~96−99% stable in the most biologically relevant environment (Opti-MEM), comparable to the polypyridyl complexes.

Singlet Oxygen Generation. As emission studies demonstrated that **6**−**10** possessed excited states with sufficient energy (>94 kJ mol^{-1})[4c] (Table S8) to sensitize $^3O_2$, the capacity of the complexes to generate $^1O_2$ was determined by measuring its phosphorescence at 1275 nm (Figure 1B). Isoabsorptive solutions were tested (with absorbance of 0.2 at 450 nm) for all complexes except for **8**, which was evaluated at a concentration of 100 μM due to poor absorbance of the complex at 450 nm. The complexes were tested as CD_3OD solutions under air; CD_3OD was used to enhance $^1O_2$ generation, increasing the likelihood that it would be sufficient to detect via luminescence.[46] $[Ru(bpy)_3]^{2+}$ was used as a positive control.[46] Despite the sufficient energy (183−193 kJ mol^{-1}) of their excited states, no signal for $^1O_2$ was detected for **6**, and complex **7** showed a very weak signal, which agrees with the short excited-state lifetimes of **6** and **7**. In contrast, all NHC complexes generated detectable $^1O_2$. The signal at 1275 nm was strongest for **9**, and the signals obtained with **8** and **10** were similar to one another. Complexes **9** and **10** have similar excited-state energies (196 and 192 kJ mol^{-1}, respectively), but **9** produced the higher signal for $^1O_2$. This difference is attributed to the longer excited-state lifetime of **9**. Complex **8** had the highest excited-state energy (225 kJ mol^{-1}), but due to the differences in concentration, it cannot be directly compared to **9** and **10**. Despite **9** generating the highest signal for the NHC complexes, it was still approximately half that of $[Ru(bpy)_3]^{2+}$.

DNA Damage. The ability of compounds **6**−**10** to alter the structure of nucleic acids with and without irradiation was evaluated by gel electrophoresis (Figure 3A). No distinguishable interactions were observed with plasmid DNA in the absence of light, which agrees with previous reports that indicated low affinity interactions for **6**,[47] with binding occurring primarily through electrostatic forces as opposed to intercalation. The electrostatic association is likely similar for **6**, **8**, and **10** since these complexes are positively charged, in contrast to the neutral, carboxylate-containing complexes **7** and **9**.

Complexes **8**−**10** were able to induce single strand breaks upon light irradiation, though all were less potent than $[Ru(bpy)_3]^{2+}$. To elucidate the reactive species responsible for these single strand breaks, experiments were performed that utilized ROS quenchers. These quenchers included 2,2,6,6-tetramethylpiperidine-1-oxyl (TEMPO), which was used to inhibit the activity of radical species;[48] sodium azide (NaN_3), which was used as a $^1O_2$ scavenger;[49] sodium pyruvate, which was used to quench hydrogen peroxide (H_2O_2);[50] and sodium iodide (NaI),[51] which was employed to scavenge hydroxyl radicals. An excess of each quencher was used with each complex, and the amount of relaxed circular DNA versus supercoiled DNA was compared. Preliminary experiments with **8**−**10** showed TEMPO was the most efficient quencher for the three NHC complexes, with a decrease (10−24%) in the formation of single strand breaks compared to the reference mixture (Figure S21). The NaI also exhibited some degree of success as a quencher, with 10−15% decrease in DNA damage

https://dx.doi.org/10.1021/acs.inorgchem.0c00686
Inorg. Chem. 2020, 59, 8882−8892

for **8**−**10**. Sodium pyruvate was largely ineffective and showed a decrease in DNA damage of <10% for **8**. Experiments with NaN_3 were inconclusive, with inconsistent effects for compound **8** versus compounds **9** and **10**. While DNA damage studies using such quenchers are known to be qualitative at best, and the quenchers are not entirely selective for individual ROS,[49] these data suggest DNA damage primarily through a radical mechanism. The quenching with TEMPO suggests a possibility for carbon-based radicals,[48] while the NaI suggests there is also the possibility for hydroxyl radicals. Given the low yield of $^1O_2$ measured by emission studies, we tentatively propose an electron-transfer-mediated mechanism. More detailed studies are planned for the future.

Cytotoxicity Assays. Ligands **1**−**5** and their corresponding complexes **6**−**10** were screened for cytotoxicity in the human promyelocytic HL60 cell line (Table 3 and Table S6). All complexes were evaluated both in the dark and with activation using 405 nm and indigo (~450 nm) light sources to evaluate their potential for light-induced anticancer activity. As the ligands do not absorb visible light, they were screened without light activation. The possible toxicity of the light sources alone, in the absence of complexes, was addressed by including a no-compound control for each experiment performed in both dark and light; this is shown as our lowest concentration dose point.

The tpy ligands **1** and **2** were potent cytotoxins, with IC_{50} values of 0.8 and 2.3 μM (Table S6). This is 36-fold greater than the cytotoxicity value for **1** reported in the HeLa cell line,[10d] but it is also up to 9-fold less potent than has been reported for a variety of other cell lines.[52,53] The potency of **2** was 22-fold greater than previously reported.[10d] The range of values observed for **1** and **2** is potentially due to a variety of factors, including different cell lines (six cell lines in total, including this report) with differing source tissue type and/or morphology, variations in incubation time (72 h vs 44 h[10d] and 48 h[53]),[4c] and the possibility of solubility issues, impeding interpretation of the notably large variation in IC_{50} values. Unlike the tpy ligands, all of the cationic imidazolium preligand salts **3**−**5** were nontoxic, with IC_{50} values >100 μM. The difference between tpy ligands **1** and **2** and NHCs **3**−**5** may be associated with the cationic and less lipophilic nature of **3**−**5**. However, there are likely more nuanced structural factors contributing to the cytotoxicity, as the potency of different terpyridine analogs can range >100 μM.[53,54]

Drastic shifts in potency were found upon coordination of the ligands to the Ru(II) center (Table 3, Figure 3B−E). Complex **6** showed minimal toxicity in the absence or presence of all light sources used, with an IC_{50} value of ~50−60 μM, and complex **7** was nontoxic. The absence of toxicity with light exposure is in agreement with the low $^1O_2$ generation of **6** and **7** and is very similar to reports of other Ru(II) terpyridine complexes.[10d,55] In the absence of light, **8**−**10** were nontoxic up to 300 μM (Table 3, Figure 3). This lack of dark toxicity is in contrast to similar bis-tridentate NHC Ru(II) complexes, which showed moderate (18.46−22.7 μM)[56] to high (0.06−1.25 μM)[57] cytotoxicity, depending on the NHC ligand used. In addition, there is a difference in hydrophobic character due to the use of PF_6^- counterions in the previous reports compared to the more hydrophilic complexes containing Cl^- counterions reported here, which also could contribute to the variation in biological activity.

Complexes **8**−**10** demonstrated significant light-dependent cytotoxicity, as irradiation resulted in IC_{50} values of 12.5 and 3.5 μM for **8** and **9**, respectively (with 405 nm light). In contrast, little enhancement in cytotoxicity was seen with compound **10** (IC_{50} ~ 70 μM). The 450 nm source produced significant cytotoxicity for **9** and **10** (IC_{50} = 5.6 and 9.1 μM, respectively) but had no effect on **8**. The difference in activity with the two light sources is attributed to a mixture of two factors: (1) variation in the absorbance at the excitation wavelength (Figure 1A), and (2) the excited-state lifetimes of the complexes (Figure 4). For example, the excited-state

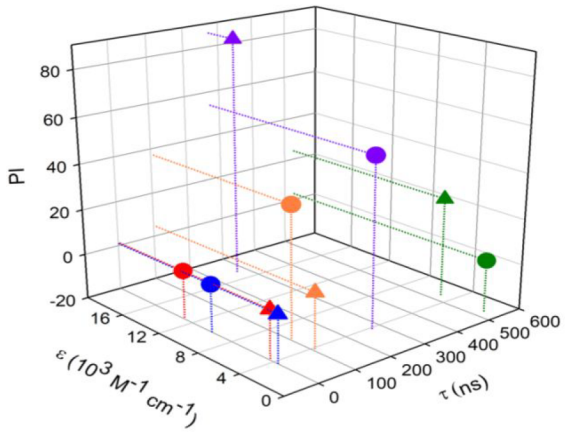

Figure 4. Dependence of phototoxicity index (PI) on lifetime (τ) and attenuation coefficient (ε; at 405 nm (triangles) and 450 nm (circles)). Compound **6** (blue), **7** (red), **8** (green), **9** (purple), and **10** (orange). The PI of compounds **8**−**10** was dependent on ε, but there was no effect for compounds **6** and **7**.

lifetime of **8** (529 ns) is ~2-fold greater than that of **9** (272 ns), which in many cases would suggest a higher potency; however, **9** is more potent when activated with either 405 or 450 nm light sources. This is likely due largely to **9** having higher attenuation coefficients than **8** at both 405 nm (ε = 17000 vs 5000 M^{-1} cm^{-1}) and 450 nm (ε = 3800 vs 1200 M^{-1} cm^{-1}).

Alternatively, the importance of the exited-state lifetime is demonstrated by the comparison of **9** and **10**. Both **9** and **10** have the same attenuation coefficient (3800 M^{-1} cm^{-1}) at 450 and 405 nm, respectively; however, **9** has a much greater potency when activated at 450 nm than **10** has when activated at 405 nm. This can be partly explained by **9** having an excited-state lifetime that is 2.5-fold greater than the excited state lifetime of **10**. This point is further supported by the substantially improved photocytotoxicity of **8**−**10** compared to those of **6** and **7**, which have much higher attenuation coefficient at 450 nm than **8**−**10** (ε = 10000 and 13000 M^{-1} cm^{-1}, respectively) but have excited state lifetimes <5 ns in water. Other properties, such as cellular uptake and localization, may also be partly responsible and will be investigated to more fully understand the differences between the phototoxicity of these compounds.

The absence of dark toxicity for **8**−**10**, combined with low micromolar cytotoxicity with irradiation, gave significant PI values. When **8** was activated with 405 nm light, a PI value > 24 was obtained. Compound **9** gave the highest PI values for 405 and 450 nm (>86 and >54, respectively), and **10** gave a respectable PI of >34 for 450 nm light. Each of these systems shows promise for PDT applications.

The low micromolar light-induced cytotoxicity of **8**−**10** is appealing when compared to the FDA-approved PDT[4c] agent,

https://dx.doi.org/10.1021/acs.inorgchem.0c00686
Inorg. Chem. 2020, 59, 8882−8892

5-aminolevulinic acid (ALA), cisplatin, and $[Ru(bpy)_3]^{2+}$. The activity of **8**–**10** was comparable or better than that of ALA, depending on which light sources were used. The potency of **9** when activated with 405 nm light was essentially the same (3.4 vs 3.5 μM) as cisplatin. When activated with 405 nm light, the IC_{50} of $[Ru(bpy)_3]^{2+}$ (5.2 μM) was between that of **8** and **9**. Complexes **9** and **10** were very effective with 450 nm light (5.6 and 9.1 μM, respectively), though $[Ru(bpy)_3]^{2+}$ was significantly more potent (0.3 μM). However, $[Ru(bpy)_3]^{2+}$ was chosen as the prototypical bidentate D_3 complex with a well-known ability to generate $^1O_2$[46] and was anticipated to be superior to the tridentate complexes. When **8**–**10** are compared to the structurally analogous tpy complexes, **6** and **7**, it is clear the inclusion of NHC ligands has a significant positive effect on photocytotoxicity. The low micromolar IC_{50} values for **9** and **10** make them superior to previously reported tpy-based complexes[10d,28a] and competitive with or superior to many reported tris-bidentate Ru(II) complexes.[3c,16a,58]

CONCLUSION

Most polypyridyl Ru(II) complexes developed for photo-therapeutic applications are chiral, and as a result, there is an intrinsic danger that the enantiomers will display different biological activities due to different interactions with chiral biological targets. The use of symmetric bis-tridentate Ru(II) complexes prevents the generation of any isomers, but until now, such structures failed to possess appropriate photo-physical characteristics for use in biological applications. Here, we demonstrate that the inclusion of tridentate NHC ligands creates Ru(II) polypyridyl complexes with excited-state lifetimes in aerated water that are 425–2116-fold longer than $[Ru(tpy)_2]^{2+}$. Moreover, one complex exhibited a longer lifetime than $[Ru(bpy)_3]^{2+}$. Complexes **8**, **9**, and **10** exhibited low micromolar light-induced cytotoxicity, while analogous tpy systems **6** and **7** showed no improvement in cytotoxicity from light irradiation. Compound **9** was the most versatile complex, as it could be activated with either 405 or 450 nm light, while **8** and **10** required excitation with either 405 or 450 nm light, respectively, consistent with their absorption profiles. The high potency of **8**–**10** makes them competitive with many of the more popular bidentate D_3 and C_2 complexes previously reported,[3c,16a,58] and, to the best of our knowledge, they are the most potent light activated Ru(II) tridentate complexes reported thus far.[10c,d] Further, **8**–**10** are the first examples of using NHCs to rationally design phototoxic Ru(II) complexes by modulating photophysical properties. Despite **10** being chiral, it serves as an important demonstration of one approach to red-shift the absorbance maxima of these systems while maintaining a long excited-state lifetime. Ideally, future systems will need to be able to absorb longer wavelength light to come closer to an ideal photosensitizer[1] while also remaining achiral. We speculate that combining tridentate NHCs with a ligand with lower energy LUMOs, such as **2**, could give both a complex with better absorbance properties[23] and a sufficiently long lifetime while remaining achiral. The conjecture can also be made that complexes with push–pull substituted ligands could also produce complexes with better absorbance properties, since these NHC complexes appear to be very sensitive to electronic changes. With this demonstration that NHCs can be incorporated in metal complexes for PDT applications, we suggest that the wide diversity of structures and properties of NHCs makes this class of compounds a particularly rich area to mine for medicinal inorganic chemistry.

ASSOCIATED CONTENT

Supporting Information

The Supporting Information is available free of charge at https://pubs.acs.org/doi/10.1021/acs.inorgchem.0c00686.

General information on synthetic methods, compound characterization, photochemical and photobiological analysis, and additional figures (PDF)

Accession Codes

CCDC 1975803–1975805 contain the supplementary crystallographic data for this paper. These data can be obtained free of charge via www.ccdc.cam.ac.uk/data_request/cif, or by emailing data_request@ccdc.cam.ac.uk, or by contacting The Cambridge Crystallographic Data Centre, 12 Union Road, Cambridge CB2 1EZ, UK; fax: +44 1223 336033.

AUTHOR INFORMATION

Corresponding Authors

Edith C. Glazer − *Department of Chemistry, University of Kentucky, Lexington, Kentucky 40506, United States;* orcid.org/0000-0002-0190-7742; Email: ec.glazer@uky.edu

John P. Selegue − *Department of Chemistry, University of Kentucky, Lexington, Kentucky 40506, United States;* orcid.org/0000-0002-1398-9474; Email: selegue@uky.edu

Authors

Raphael T. Ryan − *Department of Chemistry, University of Kentucky, Lexington, Kentucky 40506, United States*

Kimberly C. Stevens − *Department of Chemistry, University of Kentucky, Lexington, Kentucky 40506, United States*

Rosemary Calabro − *Department of Chemistry, University of Kentucky, Lexington, Kentucky 40506, United States;* orcid.org/0000-0001-9394-5385

Sean Parkin − *Department of Chemistry, University of Kentucky, Lexington, Kentucky 40506, United States;* orcid.org/0000-0001-5777-3918

Jumanah Mahmoud − *Department of Chemistry, University of Kentucky, Lexington, Kentucky 40506, United States*

Doo Young Kim − *Department of Chemistry, University of Kentucky, Lexington, Kentucky 40506, United States;* orcid.org/0000-0002-6095-5023

David K. Heidary − *Department of Chemistry, University of Kentucky, Lexington, Kentucky 40506, United States*

Complete contact information is available at: https://pubs.acs.org/10.1021/acs.inorgchem.0c00686

Notes

The authors declare no competing financial interest.

ACKNOWLEDGMENTS

We gratefully acknowledge the Kentucky Science and Engineering Foundation (KSEF-4003-RDE-020) and the National Institutes of Health (GM107586) for the support of this research. Crystallographic work was made possible by the National Science Foundation (NSF) MRI program, grants CHE-0319176 and CHE-1625732.

REFERENCES

(1) Agostinis, P.; Berg, K.; Cengel, K. A.; Foster, T. H.; Girotti, A. W.; Gollnick, S. O.; Hahn, S. M.; Hamblin, M. R.; Juzeniene, A.; Kessel, D.; Korbelik, M.; Moan, J.; Mroz, P.; Nowis, D.; Piette, J.;

Wilson, B. C.; Golab, J. Photodynamic therapy of cancer: an update. *Ca-Cancer J. Clin.* **2011**, *61* (4), 250−81.
(2) Luciano, M.; Bruckner, C. Modifications of Porphyrins and Hydroporphyrins for Their Solubilization in Aqueous Media. *Molecules* **2017**, *22* (6), 980.
(3) (a) Stacey, O. J.; Pope, S. J. A. New avenues in the design and potential application of metal complexes for photodynamic therapy. *RSC Adv.* **2013**, *3* (48), 25550−25564. (b) Lucky, S. S.; Soo, K. C.; Zhang, Y. Nanoparticles in photodynamic therapy. *Chem. Rev.* **2015**, *115* (4), 1990−2042. (c) Liu, J.; Zhang, C.; Rees, T. W.; Ke, L.; Ji, L.; Chao, H. Harnessing ruthenium(II) as photodynamic agents: Encouraging advances in cancer therapy. *Coord. Chem. Rev.* **2018**, *363*, 17−28.
(4) (a) Mari, C.; Pierroz, V.; Ferrari, S.; Gasser, G. Combination of Ru(II) complexes and light: new frontiers in cancer therapy. *Chem. Sci.* **2015**, *6* (5), 2660−2686. (b) Heinemann, F.; Karges, J.; Gasser, G. Critical Overview of the Use of Ru(II) Polypyridyl Complexes as Photosensitizers in One-Photon and Two-Photon Photodynamic Therapy. *Acc. Chem. Res.* **2017**, *50* (11), 2727−2736. (c) Monro, S.; Colon, K. L.; Yin, H.; Roque, J., 3rd; Konda, P.; Gujar, S.; Thummel, R. P.; Lilge, L.; Cameron, C. G.; McFarland, S. A. Transition Metal Complexes and Photodynamic Therapy from a Tumor-Centered Approach: Challenges, Opportunities, and Highlights from the Development of TLD1433. *Chem. Rev.* **2019**, *119* (2), 797−828. (d) Thota, S.; Rodrigues, D. A.; Crans, D. C.; Barreiro, E. J. Ru(II) Compounds: Next-Generation Anticancer Metallotherapeutics? *J. Med. Chem.* **2018**, *61* (14), 5805−5821.
(5) Dickerson, M.; Sun, Y.; Howerton, B.; Glazer, E. C. Modifying charge and hydrophilicity of simple Ru(II) polypyridyl complexes radically alters biological activities: old complexes, surprising new tricks. *Inorg. Chem.* **2014**, *53* (19), 10370−7.
(6) (a) Kalyanasundaram, K. Photophysics, photochemistry and solar energy conversion with tris(bipyridyl)ruthenium(II) and its analogues. *Coord. Chem. Rev.* **1982**, *46*, 159−244. (b) Juris, A.; Balzani, V.; Barigelletti, F.; Campagna, S.; Belser, P.; von Zelewsky, A. Ru(II) polypyridine complexes: photophysics, photochemistry, eletrochemistry, and chemiluminescence. *Coord. Chem. Rev.* **1988**, *84*, 85−277.
(7) Theralas. Press Release; September 4, 2019; https://theralase.com/pressrelease/theralase-annouces-first-patient-treated-in-phase-ii-non-muscle-invasive-bladder-cancer-clinical-study/ (accessed Sep 13, 2019).
(8) Abrahamse, H.; Hamblin, M. R. New photosensitizers for photodynamic therapy. *Biochem. J.* **2016**, *473* (4), 347−64.
(9) (a) Lincoln, R.; Kohler, L.; Monro, S.; Yin, H.; Stephenson, M.; Zong, R.; Chouai, A.; Dorsey, C.; Hennigar, R.; Thummel, R. P.; McFarland, S. A. Exploitation of long-lived ^{3}IL excited states for metal-organic photodynamic therapy: verification in a metastatic melanoma model. *J. Am. Chem. Soc.* **2013**, *135* (45), 17161−75. (b) Shi, G.; Monro, S.; Hennigar, R.; Colpitts, J.; Fong, J.; Kasimova, K.; Yin, H.; DeCoste, R.; Spencer, C.; Chamberlain, L.; Mandel, A.; Lilge, L.; McFarland, S. A. Ru(II) dyads derived from α-oligothiophenes: A new class of potent and versatile photosensitizers for PDT. *Coord. Chem. Rev.* **2015**, *282*−*283*, 127−138.
(10) (a) Zhao, R.; Hammitt, R.; Thummel, R. P.; Liu, Y.; Turro, C.; Snapka, R. M. Nuclear targets of photodynamic tridentate ruthenium complexes. *Dalton Trans.* **2009**, *48*, 10926−31. (b) Liu, Y.; Hammitt, R.; Lutterman, D. A.; Joyce, L. E.; Thummel, R. P.; Turro, C. Ru(II) Complexes of New Tridentate Ligands: Unexpected High Yield of Sensitized $^1O_2$. *Inorg. Chem.* **2009**, *48* (1), 375−385. (c) Frei, A.; Rubbiani, R.; Tubafard, S.; Blacque, O.; Anstaett, P.; Felgentrager, A.; Maisch, T.; Spiccia, L.; Gasser, G. Synthesis, characterization, and biological evaluation of new Ru(II) polypyridyl photosensitizers for photodynamic therapy. *J. Med. Chem.* **2014**, *57* (17), 7280−92. (d) Karges, J.; Blacque, O.; Jakubaszek, M.; Goud, B.; Goldner, P.; Gasser, G. Systematic investigation of the antiproliferative activity of a series of ruthenium terpyridine complexes. *J. Inorg. Biochem.* **2019**, *198*, 110752.
(11) Winkler, J. R.; Netzel, T. L.; Creutz, C.; Sutin, N. Direct observation of metal-to-ligand charge-transfer (MLCT) excited states of pentaammineruthenium(II) complexes. *J. Am. Chem. Soc.* **1987**, *109* (8), 2381−2392.
(12) Pal, A. K.; Hanan, G. S. Design, synthesis and excited-state properties of mononuclear Ru(II) complexes of tridentate heterocyclic ligands. *Chem. Soc. Rev.* **2014**, *43* (17), 6184−97.
(13) Liegghio, R.; Potvin, P. G.; Lever, A. B. P. 2,6-Dipyrazinylpyridines and Their Ruthenium(II) Complexes: A New Polynucleating Ligand Family. *Inorg. Chem.* **2001**, *40* (22), 5485−5486.
(14) (a) Howerton, B. S.; Heidary, D. K.; Glazer, E. C. Strained ruthenium complexes are potent light-activated anticancer agents. *J. Am. Chem. Soc.* **2012**, *134* (20), 8324−7. (b) Wachter, E.; Heidary, D. K.; Howerton, B. S.; Parkin, S.; Glazer, E. C. Light-activated ruthenium complexes photobind DNA and are cytotoxic in the photodynamic therapy window. *Chem. Commun.* **2012**, *48* (77), 9649−51. (c) Hidayatullah, A. N.; Wachter, E.; Heidary, D. K.; Parkin, S.; Glazer, E. C. Photoactive Ru(II) complexes with dioxinophenanthroline ligands are potent cytotoxic agents. *Inorg. Chem.* **2014**, *53* (19), 10030−2. (d) Kohler, L.; Nease, L.; Vo, P.; Garofolo, J.; Heidary, D. K.; Thummel, R. P.; Glazer, E. C. Photochemical and Photobiological Activity of Ru(II) Homoleptic and Heteroleptic Complexes Containing Methylated Bipyridyl-type Ligands. *Inorg. Chem.* **2017**, *56* (20), 12214−12223. (e) Havrylyuk, D.; Heidary, D. K.; Nease, L.; Parkin, S.; Glazer, E. C. Photochemical Properties and Structure-Activity Relationships of Ru(II) Complexes with Pyridylbenzazole Ligands as Promising Anticancer Agents. *Eur. J. Inorg. Chem.* **2017**, *2017* (12), 1687−1694.
(15) (a) Medlycott, E. A.; Hanan, G. S. Synthesis and properties of mono- and oligo-nuclear Ru(II) complexes of tridentate ligands: The quest for long-lived excited states at room temperature. *Coord. Chem. Rev.* **2006**, *250* (13−14), 1763−1782. (b) Hofmeier, H.; Schubert, U. S. Recent developments in the supramolecular chemistry of terpyridine-metal complexes. *Chem. Soc. Rev.* **2004**, *33* (6), 373−99. (c) Baranoff, E.; Collin, J. P.; Flamigni, L.; Sauvage, J. P. From ruthenium(II) to iridium(III): 15 years of triads based on bis-terpyridine complexes. *Chem. Soc. Rev.* **2004**, *33* (3), 147−55.
(16) (a) Poynton, F. E.; Bright, S. A.; Blasco, S.; Williams, D. C.; Kelly, J. M.; Gunnlaugsson, T. The development of ruthenium(II) polypyridyl complexes and conjugates for in vitro cellular and in vivo applications. *Chem. Soc. Rev.* **2017**, *46* (24), 7706−7756. (b) Wang, Y.; Huang, H.; Zhang, Q.; Zhang, P. Chirality in metal-based anticancer agents. *Dalton Trans.* **2018**, *47* (12), 4017−4026.
(17) Hua, X.; von Zelewsky, A. Enantiomerically Pure Chiral Ru^{II}(L-L)$_2$ Building Blocks for Coordination Compounds. *Inorg. Chem.* **1995**, *34* (23), 5791−5797.
(18) (a) Sun, P.; Krishnan, A.; Yadav, A.; Singh, S.; MacDonnell, F. M.; Armstrong, D. W. Enantiomeric Separations of Ruthenium(II) Polypyridyl Complexes Using High-Performance Liquid Chromatography (HPLC) with Cyclodextrin Chiral Stationary Phases (CSPs). *Inorg. Chem.* **2007**, *46* (24), 10312−10320. (b) Sun, P.; Krishnan, A.; Yadav, A.; MacDonnell, F. M.; Armstrong, D. W. Enantioseparations of Chiral Ruthenium(II) Polypyridyl Complexes Using HPLC with Macrocyclic Glycopeptide Chiral Stationary Phases (CSPs). *J. Mol. Struct.* **2008**, *890* (1−3), 75−80.
(19) (a) Brown, D. G.; Sanguantrakun, N.; Schulze, B.; Schubert, U. S.; Berlinguette, C. P. Bis(tridentate) ruthenium-terpyridine complexes featuring microsecond excited-state lifetimes. *J. Am. Chem. Soc.* **2012**, *134* (30), 12354−7. (b) Abrahamsson, M.; Jäger, M.; Österman, T.; Eriksson, L.; Persson, P.; Becker, H.-C.; Johansson, O.; Hammarström, L. A 3.0 μs Room Temperature Excited State Lifetime of a Bistridentate Ru^{II}−Polypyridine Complex for Rod-like Molecular Arrays. *J. Am. Chem. Soc.* **2006**, *128* (39), 12616−12617. (c) Abrahamsson, M.; Jäger, M.; Kumar, R. J.; Österman, T.; Persson, P.; Becker, H.-C.; Johansson, O.; Hammarström, L. Bistridentate Ruthenium(II)polypyridyl-Type Complexes with Microsecond ^{3}MLCT State Lifetimes: Sensitizers for Rod-Like Molecular Arrays. *J. Am. Chem. Soc.* **2008**, *130* (46), 15533−15542. (d) Son, S. U.; Park, K. H.; Lee, Y.-S.; Kim, B. Y.; Choi, C. H.; Lah, M. S.; Jang, Y. H.; Jang,

https://dx.doi.org/10.1021/acs.inorgchem.0c00686
Inorg. Chem. 2020, 59, 8882−8892

D.-J.; Chung, Y. K. Synthesis of Ru(II) Complexes of N-Heterocyclic Carbenes and Their Promising Photoluminescence Properties in Water. *Inorg. Chem.* **2004**, *43* (22), 6896−6898. (e) Fang, Y.-Q.; Taylor, N. J.; Hanan, G. S.; Loiseau, F.; Passalacqua, R.; Campagna, S.; Nierengarten, H.; Dorsselaer, A. V. A Strategy for Improving the Room-Temperature Luminescence Properties of Ru(II) Complexes with Tridentate Ligands. *J. Am. Chem. Soc.* **2002**, *124* (27), 7912−7913. (f) Schramm, F.; Meded, V.; Fliegl, H.; Fink, K.; Fuhr, O.; Qu, Z.; Klopper, W.; Finn, S.; Keyes, T. E.; Ruben, M. Expanding the Coordination Cage: A Ruthenium(II)−Polypyridine Complex Exhibiting High Quantum Yields under Ambient Conditions. *Inorg. Chem.* **2009**, *48* (13), 5677−5684.

(20) The greater than 1 singlet oxygen quantum yield may indicate that other unknown photochemical processes are taking place for the homoleptic complex.

(21) The pH of the water dispensed from our Milli-Q water purification system is approximately 9, and the water was used as dispensed.

(22) Kim, H.-M.; Jeong, D.; Noh, H. C.; Kang, Y. K.; Chung, Y. K. Manipulation of Absorption Maxima by Controlling Oxidation Potentials in Bis(tridentate) Ru(II) N-Heterocyclic Carbene Complexes. *Bull. Korean Chem. Soc.* **2014**, *35* (2), 448−456.

(23) Park, H. J.; Kim, K. H.; Choi, S. Y.; Kim, H. M.; Lee, W. I.; Kang, Y. K.; Chung, Y. K. Unsymmetric Ru(II) complexes with N-heterocyclic carbene and/or terpyridine ligands: synthesis, characterization, ground- and excited-state electronic structures and their application for DSSC sensitizers. *Inorg. Chem.* **2010**, *49* (16), 7340−52.

(24) Stublla, A.; Potvin, P. G. Ruthenium(II) Complexes of Carboxylated Terpyridines and Dipyrazinylpyridines. *Eur. J. Inorg. Chem.* **2010**, *2010* (19), 3040−3050.

(25) Naziruddin, A. R.; Kuo, C.-L.; Lin, W.-J.; Lo, W.-H.; Lee, C.-S.; Sun, B.-J.; Chang, A. H. H.; Hwang, W.-S. Ruthenium Complexes Bearing Unsymmetric CNC′ Pincer Ligands: Molecular Structures and Electronic Properties. *Organometallics* **2014**, *33* (10), 2575−2582.

(26) Hopkinson, M. N.; Richter, C.; Schedler, M.; Glorius, F. An overview of N-heterocyclic carbenes. *Nature* **2014**, *510* (7506), 485−96.

(27) Gaiddon, C.; Pfeffer, M. The Fate of Cycloruthenated Compounds: From C-H Activation to Innovative Anticancer Therapy. *Eur. J. Inorg. Chem.* **2017**, *2017* (12), 1639−1654.

(28) (a) Aher, S. B.; Muskawar, P. N.; Thenmozhi, K.; Bhagat, P. R. Recent developments of metal N-heterocyclic carbenes as anticancer agents. *Eur. J. Med. Chem.* **2014**, *81*, 408−19. (b) Liu, W.; Gust, R. Update on metal N-heterocyclic carbene complexes as potential antitumor metallodrugs. *Coord. Chem. Rev.* **2016**, *329*, 191−213.

(29) (a) Li, Y.; Liu, B.; Lu, X. R.; Li, M. F.; Ji, L. N.; Mao, Z. W. Cyclometalated iridium(III) N-heterocyclic carbene complexes as potential mitochondrial anticancer and photodynamic agents. *Dalton Trans.* **2017**, *46* (34), 11363−11371. (b) Li, Y.; Tan, C. P.; Zhang, W.; He, L.; Ji, L. N.; Mao, Z. W. Phosphorescent iridium(III)-bis-N-heterocyclic carbene complexes as mitochondria-targeted theranostic and photodynamic anticancer agents. *Biomaterials* **2015**, *39*, 95−104. (c) Zou, T.; Lok, C. N.; Fung, Y. M.; Che, C. M. Luminescent organoplatinum(II) complexes containing bis(N-heterocyclic carbene) ligands selectively target the endoplasmic reticulum and induce potent photo-toxicity. *Chem. Commun.* **2013**, *49* (47), 5423−5. (d) Liu, B.; Monro, S.; Jabed, M. A.; Cameron, C. G.; Colon, K. L.; Xu, W.; Kilina, S.; McFarland, S. A.; Sun, W. Neutral iridium(III) complexes bearing BODIPY-substituted N-heterocyclic carbene (NHC) ligands: synthesis, photophysics, in vitro theranostic photodynamic therapy, and antimicrobial activity. *Photochem. Photobiol. Sci.* **2019**, *18* (10), 2381−2396. (e) Hung, F. F.; Wu, S. X.; To, W. P.; Kwong, W. L.; Guan, X.; Lu, W.; Low, K. H.; Che, C. M. Palladium(II) Acetylide Complexes with Pincer-Type Ligands: Photophysical Properties, Intermolecular Interactions, and Photocytotoxicity. *Chem. - Asian J.* **2017**, *12* (1), 145−158.

(30) (a) Wadman, S. H.; Lutz, M.; Tooke, D. M.; Spek, A. L.; Hartl, F.; Havenith, R. W. A.; van Klink, G. P. M.; van Koten, G. Consequences of N,C,N′- and C,N,N′-Coordination Modes on Electronic and Photophysical Properties of Cyclometalated Aryl Ruthenium(II) Complexes. *Inorg. Chem.* **2009**, *48* (5), 1887−1900. (b) Lashgari, K.; Kritikos, M.; Norrestam, R.; Norrby, T. Bis(terpyridine)ruthenium(II) bis(hexafluorophosphate) diacetonitrile solvate. *Acta Crystallogr., Sect. C: Cryst. Struct. Commun.* **1999**, *55* (1), 64−67.

(31) Kershaw Cook, L. J.; Halcrow, M. A. Doping ruthenium complexes into a molecular spin-crossover material. *Polyhedron* **2015**, *87*, 91−97.

(32) Previously, the structure of **8** had to be solved as the tetraphenylborate salt, due to disorder precluding solving the structure as the hexafluorophosphate salt. See ref 19d. Here, we report for the first time the structure of **8** as the hexafluorophosphate salt.

(33) (a) Lee, C.-S.; Zhuang, R. R.; Wang, J.-C.; Hwang, W.-S.; Lin, I. J. B. Proton-Sensitive Luminescent Ruthenium(II) Complexes with Pyrazine-Based Pincer-Type N-Heterocyclic Carbene Ligands. *Organometallics* **2012**, *31* (14), 4980−4987. (b) Shee, S.; Paul, B.; Kundu, S. Counter Anion Controlled Reactivity Switch in Transfer Hydrogenation: A Case Study between Ketones and Nitroarenes. *ChemistrySelect* **2017**, *2* (4), 1705−1710. (c) Gu, S.; Liu, B.; Chen, J.; Wu, H.; Chen, W. Synthesis, structures, and properties of ruthenium(II) complexes of N-(1,10-phenanthrolin-2-yl)-imidazolylidenes. *Dalton Trans.* **2012**, *41* (3), 962−70.

(34) (a) Constable, E. C.; Dunphy, E. L.; Housecroft, C. E.; Neuburger, M.; Schaffner, S.; Schaper, F.; Batten, S. R. Expanded ligands: bis(2,2′:6′,2″-terpyridine carboxylic acid)ruthenium(ii) complexes as metallosupramolecular analogues of dicarboxylic acids. *Dalton Trans.* **2007**, *38*, 4323−32. (b) Potvin, P. G.; Luyen, P. U.; Bräckow, J. Electrostatic Bubbles and Supramolecular Assistance of Photosensitization by Carboxylated Ru(II) Complexes. *J. Am. Chem. Soc.* **2003**, *125* (16), 4894−4906. (c) Zadykowicz, J.; Potvin, P. G. Mono- and Dinuclear Ruthenium(II) Complexes of 2,6-Di(pyrazol-3-yl)pyridines: Deprotonation, Functionalization, and Supramolecular Association. *Inorg. Chem.* **1999**, *38* (10), 2434−2441.

(35) Nazeeruddin, M. K.; Péchy, P.; Renouard, T.; Zakeeruddin, S. M.; Humphry-Baker, R.; Comte, P.; Liska, P.; Cevey, L.; Costa, E.; Shklover, V.; Spiccia, L.; Deacon, G. B.; Bignozzi, C. A.; Grätzel, M. Engineering of Efficient Panchromatic Sensitizers for Nanocrystalline TiO2-Based Solar Cells. *J. Am. Chem. Soc.* **2001**, *123* (8), 1613−1624.

(36) Dinda, J.; Liatard, S.; Chauvin, J.; Jouvenot, D.; Loiseau, F. Electronic and geometrical manipulation of the excited state of bis-terdentate homo- and heteroleptic ruthenium complexes. *Dalton Trans.* **2011**, *40* (14), 3683−8.

(37) Schiøtt, B.; Iversen, B. B.; Madsen, G. K. H.; Larsen, F. K.; Bruice, T. C. On the electronic nature of low-barrier hydrogen bonds in enzymatic reactions. *Proc. Natl. Acad. Sci. U. S. A.* **1998**, *95* (22), 12799.

(38) The emission from the complexes is weak in water. To avoid additional Raman scattering the compounds were measured in Milli-Q water instead of a buffered solution which would have more components that could scatter light.

(39) Our measurements for **8** were almost 6-fold less than the previously reported 3100 ns lifetime, which we attributed to quenching of the excited state by oxygen as a consequence of these measurements being performed under aerobic conditions.

(40) Kreitner, C.; Heinze, K. Excited state decay of cyclometalated polypyridine ruthenium complexes: insight from theory and experiment. *Dalton Trans.* **2016**, *45* (35), 13631−47.

(41) Huynh, H. V. General Properties of Classical NHCs and Their Complexes. In *The Organometallic Chemistry of N-Heterocyclic Carbenes*; Wiley: Hoboken, NJ, 2017; pp 17−51.

(42) Sepehrifard, A.; Chen, S.; Stublla, A.; Potvin, P. G.; Morin, S. Effects of ligand LUMO levels, anchoring groups and spacers in Ru(II)-based terpyridine and dipyrazinylpyridine complexes on adsorption and photoconversion efficiency in DSSCs. *Electrochim. Acta* **2013**, *87*, 236−244.

https://dx.doi.org/10.1021/acs.inorgchem.0c00686
Inorg. Chem. 2020, 59, 8882−8892

(43) Batista, R. C.; da Silva Miranda, F.; Pinheiro, C. B.; Lanznaster, M. An Esculetin-Cobalt(III) Archetype for Redox-Activated Drug Delivery Platforms with Hypoxic Selectivity. *Eur. J. Inorg. Chem.* **2018**, *2018* (5), 612−616.
(44) Photoelectrochemical Cells for Hydrogen Generation. In *Electrochemical Technologies for Energy Storage and Conversion*, Ru-Shi Liu, L. Z., Sun, X., Liu, H., Zhang, J., Eds.; Wiley-VCH: Weinheim, Germany, 2012; Vol. 2, pp 541−599.
(45) Lai, B.-C.; Wu, J.-G.; Luo, S.-C. Revisiting Background Signals and the Electrochemical Windows of Au, Pt, and GC Electrodes in Biological Buffers. *ACS Appl. Energy Mater.* **2019**, *2* (9), 6808−6816.
(46) Garcìa-Fresnadillo, D.; Georgiadou, Y.; Orellana, G.; Braun, A. M.; Oliveros, E. Singlet-Oxygen ($^1\Delta_g$) Production by Ruthenium(II) complexes containing polyazaheterocyclic ligands in methanol and in water. *Helv. Chim. Acta* **1996**, *79* (4), 1222−1238.
(47) (a) Tossi, A. B.; Kelly, J. M. A study of some polypyridylruthenium(II) complexes as DNA binders and photocleavage reagents. *Photochem. Photobiol.* **1989**, *49* (5), 545−556. (b) Jang, Y.-J.; Lee, H.-M.; Jang, K.-J.; Lee, J.-C.; Kim, S.-K.; Cho, T.-S. Comparison of the Binding Modes of $[Ru(2,2'\text{-bipyridine})_3]^{2+}$ and $[Ru(2,2':6',2''\text{-terpyridine})_2]^{2+}$ to Native DNA. *Bull. Korean Chem. Soc.* **2010**, *31* (5), 1314−1318.
(48) Yadav, A.; Janaratne, T.; Krishnan, A.; Singhal, S. S.; Yadav, S.; Dayoub, A. S.; Hawkins, D. L.; Awasthi, S.; MacDonnell, F. M. Regression of lung cancer by hypoxia-sensitizing ruthenium polypyridyl complexes. *Mol. Cancer Ther.* **2013**, *12* (5), 643−53.
(49) Leichnitz, S.; Heinrich, J.; Kulak, N. A fluorescence assay for the detection of hydrogen peroxide and hydroxyl radicals generated by metallonucleases. *Chem. Commun.* **2018**, *54* (95), 13411−13414.
(50) Hagar, H.; Ueda, N.; Shah, S. V. Role of reactive oxygen metabolites in DNA damage and cell death in chemical hypoxic injury to LLC-PK1 cells. *Am. J. Physiol.* **1996**, *271* (1), F209−F215.
(51) Pillar-Little, T. J.; Wanninayake, N.; Nease, L.; Heidary, D. K.; Glazer, E. C.; Kim, D. Y. Superior photodynamic effect of carbon quantum dots through both type I and type II pathways: Detailed comparison study of top-down-synthesized and bottom-up-synthesized carbon quantum dots. *Carbon* **2018**, *140*, 616−623.
(52) Ligand 1 has been reported to have nanomolar IC_{50} values for A549 (250 nM), SK-OV-3 (80 nM), SK-MEL-2 (180 nM), and HCT15 (230 nM).
(53) Son, J.-K.; Zhao, L.-X.; Basnet, A.; Thapa, P.; Karki, R.; Na, Y.; Jahng, Y.; Jeong, T. C.; Jeong, B.-S.; Lee, C.-S. Synthesis of 2,6-diaryl-substituted pyridines and their antitumor activities. *Eur. J. Med. Chem.* **2008**, *43* (4), 675−682.
(54) Zhao, L.-X.; Sherchan, J.; Park, J. K.; Jahng, Y.; Jeong, B.-S.; Jeong, T. C.; Lee, C.-S.; Lee, E.-S. Synthesis, cytotoxicity and structure-activity relationship study of terpyridines. *Arch. Pharmacal Res.* **2006**, *29* (12), 1091−1095.
(55) Hahn, E. M.; Estrada-Ortiz, N.; Han, J.; Ferreira, V. F. C.; Kapp, T. G.; Correia, J. D. G.; Casini, A.; Kühn, F. E. Functionalization of Ruthenium(II) Terpyridine Complexes with Cyclic RGD Peptides To Target Integrin Receptors in Cancer Cells. *Eur. J. Inorg. Chem.* **2017**, *2017* (12), 1667−1672.
(56) Roymahapatra, G.; Dinda, J.; Mishra, A.; Mahapatra, A.; Hwang, W. S.; Mandal, S. M. Cytotoxic potency of self-assembled Ruthenium(II)-NHC complexes with pincer type 2, 6-bis(N-methylimidazolylidene/benzimidazolylidene)pyrazine ligands. *J. Cancer Res. Ther.* **2015**, *11* (1), 105−13.
(57) Dinda, J.; Adhikary, S. D.; Roymahapatra, G.; Nakka, K. K.; Santra, M. K. Synthesis, structure, electrochemistry and cytotoxicity studies of Ru(II) and Pt(II)−N-heterocyclic carbene complexes of CNC-pincer ligand. *Inorg. Chim. Acta* **2014**, *413*, 23−31.
(58) Zeng, L.; Gupta, P.; Chen, Y.; Wang, E.; Ji, L.; Chao, H.; Chen, Z. S. The development of anticancer ruthenium(II) complexes: from single molecule compounds to nanomaterials. *Chem. Soc. Rev.* **2017**, *46* (19), 5771−5804.

https://dx.doi.org/10.1021/acs.inorgchem.0c00686
Inorg. Chem. 2020, 59, 8882−8892